THE JOURNAL OF NAVIGATION (2015), **68**, 52–70.
doi:10.1017/S0373463314000538

A Beam Scanning Method based on the Helical Antenna for Space-based AIS

Yun Cheng, Lihu Chen and Xiaoqian Chen

(*College of Aerospace Science and Engineering, National University of Defense Technology, P.R. China*)
(E-mail: chenxiaoqian@nudt.edu.cn)

We investigate a strategy to address the problem of low ship detection probability of space-based Automatic Identification System (AIS). A directional AIS antenna and an innovative beam scanning method are proposed, which scan the antenna across a wide swath to provide complete coverage and maintain the advantage of a narrow footprint to reduce signal collision. Aiming at the mission requirement of global ship detection by the year 2016, the appropriate swath, the scanning range and the scanning rate were studied and designed in detail. Theoretical analysis and simulations showed that this scanning antenna can greatly improve ship detection probability and hold the detection probability at an average reporting interval from six to 15 seconds for most oceans when compared with the traditional fixed wide beam antenna. Furthermore, the detection capacity of this scanning antenna was little affected by the heights of different Low Earth Orbits. The results of this work show that the design of the helical antenna along with the beam scanning method can be considered as a building block of future space-based AIS.

KEY WORDS

1. Space-based AIS. 2. Helical antenna. 3. Beam scanning. 4. Detection probability.

Submitted: 22 January 2014. Accepted: 24 July 2014. First published online: 13 August 2014.

1. INTRODUCTION. The Universal Ship-borne Automatic Identification System (AIS) is a ship-to-ship and ship-to-shore reporting system based on broadcasting of short fixed-length Time Division Multiple Access (TDMA) messages in the maritime dedicated Very High Frequency (VHF) band. It is defined by the International Telecommunication Union (ITU, 2001). The AIS communication system was initially developed as a supplement to radar to provide navigation information to vessels and shore stations, including position, identification, course and speed over ground as well as static and voyage related information. By means of continuous traffic monitoring, vessels can anticipate and thus avoid collisions at sea (Gunnar Aarsæther and Moan, 2009; Silveira et. al., 2013). Furthermore, AIS also offers important ship monitoring services to coastguards or search and rescue organisations.

The International Convention for the Safety of Life at Sea (SOLAS) requires AIS on board passenger ships, vessels over 300 tonnes on international voyages, and vessels over 500 tonnes on non-international voyages. It became mandatory on all SOLAS ships built after 30 June 2002, and on older ships by 1 July 2008 (ITU, 2006).

Due to the limited coverage range of terrestrial AIS, space-based AIS appeared and was firstly presented at the 4th International Academy of Astronautics Symposium on Small Satellites for Earth Observation in Berlin in April 2003 (Wahl and Høye, 2003). Spaced-based AIS can cover a much broader area, hence providing a more comprehensive surveillance and management capability. Since then, the Norwegian Defence Research Establishment, Forsvarets ForsknInginstitutt (FFI) has for some time performed a feasibility study of space-based AIS reception and the prospects for conducting ocean surveillance by a space-based AIS receiver in Low Earth Orbit (LEO) (Meland et al., 2004; Carson-Jackson, 2012). Nowadays, there are several on going activities, from both space research institutes and industry to further develop and operate space-based AIS. However, as the initial AIS system is not designed for space reception, some technical challenges arise that highly limit the system performance of current demonstration AIS satellites. Our innovative "Board Nanosat" TianTuo-1 that carried the AIS receiver with two monopole antennas, successfully launched into space in May 2012, has achieved about 30% ship detection probability. The latest AIS satellite "ExactView-1", launched into orbit in July 2012, was designed to be the most advanced AIS satellite built to date and during the testing phase it lived up to that billing as it resulted in increased detection rates of up to 15% – 40% better than any of the previous satellite sensors (ExactEarth, 2013). But it is estimated that its average probability of ship detection is no more than 70%, and even lower in the high ship density regions.

Aiming at enhancing performance, many studies have been carried out and some efficient methods have been proposed by ESA, the European Commission, Canada and the United States in recent years. FFI has released a series of reports to study the model, mechanism and influencing factors of AIS reception from space. Dahl (2006) studied the space-based receiver for maritime traffic monitoring using interference cancellation, which examined receiver solutions to reduce the interference problem by utilising antenna diversity. Burzigotti et al. (2012) described an innovative receiver architecture for space-based AIS, which can provide excellent performance against noise, as well as excellent resilience to message collisions, Doppler shift and delay spread. Considering the inevitability of overlapped AIS messages, Zhu et al. (2012) proposed a blind-source separation method based on counteraction theory of antenna space to separate the mixing AIS signals. In the aspect of advanced signal processing techniques, Gallardo and Sorger (2010) proposed an innovative coherent demodulator based on Maximum Likelihood Estimation (MLE) and a Viterbi decoder to receive AIS signals from space and handle the large Doppler frequency shift. Zhang et al. (2010) proposed a set of new demodulation algorithms which combine a number of signal demodulation schemes with appropriately selected weights to detect/demodulate the desired signals in the presence of other interfering signals. For AIS antennae, a compact patch antenna was developed by Thales Systèmes Aéroportés (TSA) and Telecom ParisTech (TPT) Comelec laboratory (Dousset et al., 2012) to satisfy the size and mass limitations for space-based AIS on the small satellite platform. The German Aerospace Centre (DLR) designed a self-deploying and self-stabilising helical antenna of excellent directionality for a small AIS satellite to detect AIS messages with high

https://doi.org/10.1017/S0373463314000538 Published online by Cambridge University Press

Table 1. Global vessels requiring a Class A terminal.

Zone/year	2008	2009	2010	2011	2012	2013	2014	2015	2016
Mediterranean	7947	8194	8448	8710	8980	9258	9545	9841	10146
Pacific	15415	15983	16386	16894	17418	17958	18514	19008	19680
Atlantic	17485	18027	18585	19161	19755	20368	20999	21650	22321
Africa/Indian	13246	15365	14080	14516	14966	15430	15908	16402	16910
NorthSea/Arctic	3785	3902	4023	4147	4276	4409	4545	4686	4831
World Vessels	57878	59672	61522	63429	65395	67422	69512	71667	73889

gain and narrow footprint (Block et al., 2013). However, these two literatures mainly focus on the feasibility, electronic and structure design of the antenna and the performance of space-based AIS under these two antennae have not yet been systematically studied and verified.

As far as different measures in enhancing space-based AIS performance are concerned, the AIS antenna as the entrance of the AIS messages can be treated as the most efficient segment, compared with other methods such as receiver and signal processing algorithm. Inspired by the excellent performance of the helical antenna, this work proposes a helical antenna and a beam-scanning method based on this helical antenna to improve the performance of space-based AIS. The helical antenna has strong directionality, thus can form a narrow beam to reduce signal collisions compared with the traditional wide beam antenna. On the other hand, the beam-scanning method described in this paper can enable a large coverage area by beam-scanning during the AIS satellite moving in orbit. Combining these two merits, it is expected that the devised helical antenna along with the innovative beam-scanning method can not only enhance ship detection probability but also achieve rapid global ocean coverage.

2. GLOBAL SHIP DETECTION ANALYSIS

2.1. *Global Ship Distributions.* With ever-increasing global shipping, there are more and more ships which are mandatorily equipped with AIS terminals. In 2006 the overall ship population was estimated to be around 70 000, among which 48 500 ships were equipped with AIS Class A transmitters. Table 1 in Scorzolini et al. (2010) reported the vessels requiring an AIS Class A terminal, as reported in the past eight years and identifying a long-term growth trend of around 3·1% per year.

From Table 1, it can be seen that the number of ships in different oceans differ greatly from each other. Because the ship detection probability highly depends on the ship density, the AIS satellite with a narrow swath is more likely to obtain a high ship detection probability. Therefore, for different mission scenarios, it is necessary to analyse the ship distributions in these oceans if adopting a narrow beam antenna. The areas of these oceans are 2·50, 179·68, 91·66, 76·17 and 14·79 million km^2, corresponding to the Mediterranean, Pacific, Atlantic, Africa/Indian and North Sea/Arctic. In this work, we suppose that this antenna design is to be fitted to an AIS satellite launching in 2014 and holding a two-year working life-span to 2016.

Table 2 shows the forecasted average number of ships to 2016 in coverage with swath widths less than 800 nautical miles (NM), assuming even ship distributions.

https://doi.org/10.1017/S0373463314000538 Published online by Cambridge University Press

Table 2. Forecasted average number of ships in coverage with the swath widths of less than 800 NM.

Zone/diameter	300 NM	400 NM	500 NM	600 NM	700 NM	800 NM
Mediterranean	982	1747	2729	3930	5349	6986
Pacific	27	47	74	106	144	189
Atlantic	59	105	164	236	321	419
Africa/Indian	53	96	149	215	293	382
North Sea/Arctic	79	140	220	316	431	562

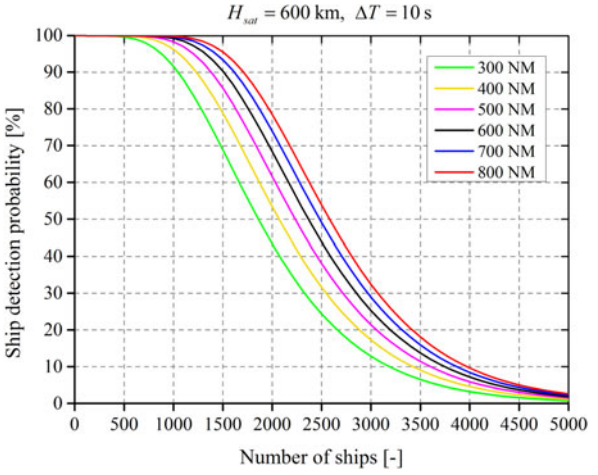

Figure 1. Ship detection probability as a function of number of ships for swath widths less than 800 NM.

The results in Table 2 show that the Mediterranean Sea has much higher ship density compared with the other four oceans.

2.2. *The Detection Probability Analysis.* Several approaches and simulation models are present in the literature to evaluate the performance of the space-based AIS system under some specific assumptions. The one Høye (2004) derived from the aspect of analyses on message collision mechanism and antenna swath width is considered to be the most accurate, even though the assumptions used to derive a formula for the ship probability of detection are quite restrictive.

The detection probability of space-based AIS for an arbitrary ship within the coverage during the observation time T_{obs} can be expressed as

$$P = 1 - \left[1 - \left(1 - \frac{1}{37{\cdot}5{\cdot}n_{ch}{\cdot}\Delta T}\right)^{(1-s)\cdot N_{tot}-1} \cdot \left(1 - \frac{2}{37{\cdot}5{\cdot}n_{ch}{\cdot}\Delta T}\right)^{s\cdot N_{tot}}\right]^{\frac{T_{obs}}{\Delta T}} \quad (1)$$

where N_{tot} is the total number of ships in the coverage area, n_{ch} is the number of independent VHF channels, ΔT is the ship average reporting interval, T_{obs} is the observation time in the satellite field of view and s is referred to as the overlap factor.

By assuming an orbit altitude of 600 km, Figure 1 shows the ship detection probability as a function of number of ships within the observation area for swath widths less than 800 NM. It includes only the Type I interference mechanism (Høye, 2006)

https://doi.org/10.1017/S0373463314000538 Published online by Cambridge University Press

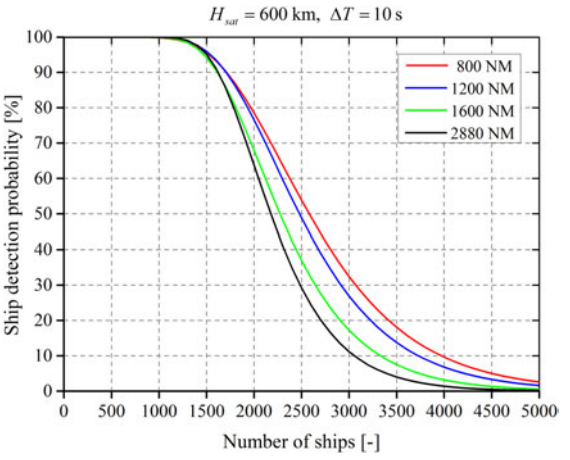

Figure 2. Ship detection probability as a function of number of ships for swath widths larger than 800 NM.

for coinciding transmissions. Figure 2 shows the ship detection probability as a function of number of ships within the observation area for swath widths larger than 800 NM. This includes both Type I and Type II interference mechanisms (Høye, 2006) for coinciding transmissions.

It can be seen that for swath widths up to 800 NM the ship detection probability increases with the increasing swath width for a given number of ships, while for swath widths larger than 800 NM the ship detection probability decreases with increasing swath width. This implies that Type II interference dominates the detection probability because there are much lower ship densities and longer observation times in the coverage of swath widths larger than 800 NM for the given number of ships. Therefore, in the real scenario, a narrow beam antenna has stronger detection capacity in high ship density regions if we do not consider the coverage area.

Comparing the average ship distributions in the last four oceans to Figure 1, it can be seen that when asked to achieve a ship detection probability of more than 80%, the appropriate swath width can be any desired value in the range from 300 NM to 800 NM. However, for the Mediterranean Sea with extremely high ship density, AIS reception in this area from space has not been very successful in the past. Only a few AIS messages can be detected and the ship detection probability tends towards zero. Obviously, it is believed that attempting to achieve very high ship detection probability in the Mediterranean Sea only by narrowing the antenna swath is not feasible. In this study, it is expected to raise the ship detection probability to 30% in one satellite overpass through a new antenna design. Then, the suitable swath width should be in the range of 300 to 500 NM as can be seen from Table 2 and Figure 1.

Finally, considering ship detection requirements on all the five sea areas studied, the candidate range of antenna swath width is from 300 NM to 500 NM when the AIS satellite moves in a 600 km LEO.

3. THE AIS ANTENNA.

As analysed in section 2.2, the antenna swath can positively influence the ship detection probability with interference, especially in high ship density regions. The solution to this problem could be using a more directional

https://doi.org/10.1017/S0373463314000538 Published online by Cambridge University Press

Table 3. Link budget parameters for AIS satellite.

Technical parameter	Typical value	Remark
Ship transmitted power P_t	> 10·8 dBW	> 12 W, Class A ships
Ship antenna gain G_{ship}	2 dBi	assumed
Transmit cable & miscellaneous losses L_t	3 dB	assumed
Free space path loss L_p	132·2 dB @600 km 139·9 dB @1450 km	$L_p = 20 \lg f + 20 \lg D + 32{\cdot}45$
Atmospheric attenuation L_a	0 dB	
Polarization loss L_{pol}	3 dB	transmit at linear polarisation, receive at circular polarisation
Satellite RF line/filter losses L_f	2·5 dB	assumed
Satellite antenna gain G_{ra}	G_{ra}	
Receiver sensitivity R_s	− 112 dBm	for 1% packet error rate
Net margin P_N	$G_{ra} + 14{\cdot}1$ (max) $G_{ra} + 6{\cdot}4$ (min)	$P_N = P_t + G_{ship} - L_t - L_p - L_a - L_{pol} - L_f + G_{ra} + R_s$

AIS antenna to limit the field of view and thereby decreasing the number of ships simultaneously visible to the AIS receiver. The traditional antenna such as monopole/dipole antenna used on satellites such as Nanosatellite Tracking of Ships (NTS), AISSat-1, TianTuo-1 has a wide swath and results in low detection probability, and is thus not feasible in this application. The helix antenna, micro-strip patch antenna and smart antenna array which can form narrow beams and hold good directionality seem to be pertinent candidates for AIS receivers. Considering the dimension and mass limitations on small satellites that usually take the AIS payload, the smart antenna array is also not applicable. A helix antenna has strong directionality, can achieve higher gain and offer a steep gain slope in its antenna pattern, which reduces the footprint size and improves the power diversity in the received signals, is thought to be preferable to micro-strip patch antenna. A series of helix antennas had been constructed and verified by DLR for their future small AIS satellite "AISat" (Block et al., 2013).

3.1. *Link Budget Calculation*. One of the most basic performance measures of satellite communication systems is the link budget. For the space-based AIS system, it consists of a calculation of the received power at the satellite from one ship and a comparison with the receiver sensitivity. Besides receiver sensitivity, several significant parameters such as ship transmitted power, ship antenna gain, transmit cable and miscellaneous losses, free space path loss, atmospheric attenuation, polarisation loss, are the most significant parameters in antenna design to obtain an adequate net margin to detect and decode AIS messages. In this work, the above parameters are shown in Table 3, and have been extracted from some AIS satellites in the past, assuming a constant gain of ship antenna.

However, AIS fitted ships usually used the half-wave dipole antenna as the ship transmitting antenna. The antenna is vertically polarised. The maximum gain for such an antenna is 2·15 dB directed in the horizontal plane of the ship. The half-power beam width is 78°. The radiation pattern for this antenna in the vertical direction is given in literature (Stutzman and Thiele, 2012) as

$$f_{0{\cdot}5\lambda}(\theta, \varphi) = \frac{\cos[(\pi/2) \cdot \cos\theta]}{\sin^2\theta} \tag{2}$$

where θ is the angle between the radiation direction and z-axis.

https://doi.org/10.1017/S0373463314000538 Published online by Cambridge University Press

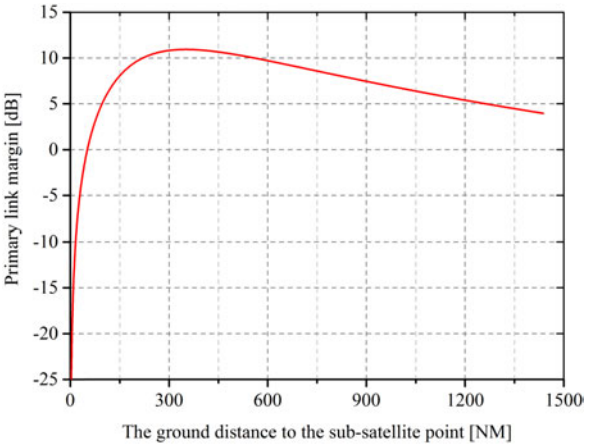

Figure 3. The primary link margin as a function of ground distance to the sub-satellite point without considering the satellite antenna gain.

Without taking account of the satellite antenna gain, the primary link margin as a function of ground distance can be estimated from the above analyses, shown in Figure 3.

As can be seen from Figure 3, the primary link margin is more than 3 dB for most ground distances except for a sharp drop around the sub-satellite point of radius ~40 NM due to the ship antenna radiation pattern. Therefore, for this study, the gain is not the determining factor in the helical antenna design due to its high gain merit. The key issue is still designing to make the swath width of the helix antenna between 300 NM and 500 NM at the 600 km altitude. This can be converted to make the beam width in the range of 50° ~ 74°.

3.2. *The Helical Antenna Design*. The monofilar axial-mode helix antenna, noncritical and one of the easiest to build, is taken as the initial choice for the AIS satellite in this study. According to antenna theory (Stutzman and Thiele, 2012), the monofilar helix antenna design can apply the following quasi-empirical formulas,

Half Power Beam Width (HPBW):

$$HPBW = \frac{65^\circ}{\frac{C}{\lambda}\sqrt{n\frac{S}{\lambda}}} \tag{3}$$

Beam Width between First Nulls (BWFN):

$$BWFN = \frac{115^\circ}{\frac{C}{\lambda}\sqrt{n\frac{S}{\lambda}}} \tag{4}$$

Gain:

$$G = 6{\cdot}2\pi\left(\frac{C}{\lambda}\right)^2 n\frac{S}{\lambda} \tag{5}$$

And, the pitch angle of the helix is

$$\alpha = \arctan(S/\pi d) \tag{6}$$

https://doi.org/10.1017/S0373463314000538 Published online by Cambridge University Press

where, C is the circumference of helix, S is the spacing between turns (centre to centre), d is the diameter of helix and n is the number of turns. λ is the wavelength of AIS signal. All these above relations have the restrictions that $12° \leqslant \alpha \leqslant 14°$, $0{\cdot}8 < C/\lambda < 1{\cdot}2$ and $n \geqslant 4$.

The AIS standard calls for an in-band signal suppression of 10 dB to avoid interference (Dahl, 2006). This means that the Field Of View (FOV) of the helical antenna should be larger than or equal to its −10 dB beam width without considering link losses due to the path differences between sub-satellite point and edge of the coverage to the AIS receiver. However, the analytic expression of −10 dB beam width of the helix antenna is hard to obtain. Here, we can firstly use the index "*BWFN*" instead of the −10 dB beam width to calculate the number of turns and the peak gain. Then if the gain is larger than 10 dBi, the number of turns should reduce gradually to make the −10 dB beam width approach its FOV by simulation. Otherwise, increasing the number of turns until the FOV of the antenna is proximal to the −10 dB beam width. By this way, a considerable performance can be achieved with the least number of turns to relax the platform limitation.

Considering these restrictions on Equations (3) through (6), the parameters generally can be set as $C/\lambda = 1$ and $\alpha = 14°$. The wavelength of the AIS signal is 1·85 m (ITU, 2001).

So the diameter of helix is

$$d = \frac{C}{\pi} = \frac{\lambda}{\pi} = 0{\cdot}589 \text{ m} \tag{7}$$

From Equation (4), the number of turns can be estimated as

$$n = (115/C_\lambda \cdot BWFN)^2/S_\lambda = (115/74)^2/0{\cdot}25 = 9{\cdot}7 \tag{8}$$

For convenience of design, the number of turns is made ten temporarily.

So, the gain can be obtained from Equation (5) as

$$G = 6{\cdot}2C_\lambda^2 nS_\lambda = 6{\cdot}2 \times 10 \times 0{\cdot}25 = 15.5 \text{ dBi} \tag{9}$$

This well exceeds the interference criteria of 10 dB. Therefore, the number of turns should decrease.

Next, using the above antenna parameters, simulations based on CST MWS (CST Microwave Studio) tool have been made to seek the optimal number of turns. By simulations, it can be obtained that the −10 dB beam width is 72·2° at $n = 7$, and 68·2° at $n = 8$. So the number of turns should be chosen as $n = 8$. The result of the gain (directivity) plot for the 8-turn helical antenna at 162 MHz is shown in Figure 4.

From this simulation, it can be found that the maximum gain in main lobe direction is 12·2 dB. The maximum gain of the side lobe gain is below 0 dB. The beam width between first nulls of the main beam is about 72·8°. The beam width of the first side lobe is larger than 120°. Therefore, AIS signals outside of the main lobe can be sufficiently suppressed due to the low side lobe gain, broad side lobe beam width and path loss far away from the main beam. Accordingly, the FOV of the designed helix antenna can be treated as 72·8°.

The theoretical gain of the 8-turn helical antenna by Equation (5) is

$$G = 6{\cdot}2C_\lambda^2 nS_\lambda = 6{\cdot}2 \times 8 \times 0{\cdot}25 = 12{\cdot}4 \text{ dBi} \tag{10}$$

https://doi.org/10.1017/S0373463314000538 Published online by Cambridge University Press

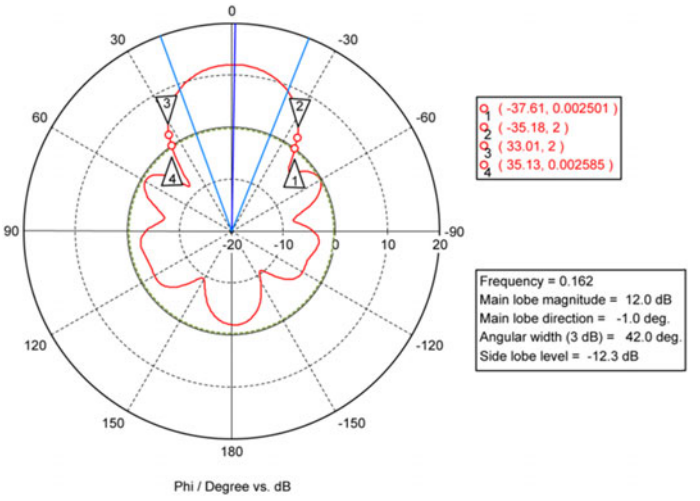

Figure 4. Simulated far-field gain plot for the 8-turn helical antenna at 162 MHz.

The full free length of the helix antenna is

$$A = nS = n{\cdot}C{\cdot}\tan\alpha = 8 \times 1{\cdot}85 \times \tan 14^\circ = 3{\cdot}7\ \text{m}$$

Obviously, the gain from simulation is in agreement with the theoretical result by quasi-empirical formulae and satisfies the gain requirement of the system, thus this design is reasonable and acceptable.

4. A BEAM SCANNING METHOD BASED ON THE HELICAL ANTENNA

4.1. *The idea of the beam scanning method.* In order to get a similar coverage area to the traditional wide beam antenna by a helical antenna, we can make the helical antenna scan reciprocatively in the direction perpendicular to the satellite velocity vector within a certain degree and this can be achieved by the Attitude Determine and Control System or a dedicated servo-control mechanism. The instantaneous scanning footprint of the helical antenna that far away from the nadir tends to be a spherical ellipse because of the round Earth surface. The beam-scanning track on the Earth's surface by the helical antenna is illustrated in Figure 5. It is not difficult to understand that if the scanning range can reach the edge of the FOV of the wide beam antenna, the helical antenna can achieve the same coverage area as the wide beam antenna, except for some blind areas near the edge of the footprints.

4.2. *The scanning range.* When discussing this beam scanning method, two key parameters are that the side swaying angle and the scanning rate should be designed carefully in order to achieve rapid global coverage and reduce the blind area. As shown in Figure 5, thanks to the round shape of the coverage, in the proximity of the sub-satellite ground track, a ship would experience the highest observation time whereas those in the borders of the antenna pattern would experience lower

https://doi.org/10.1017/S0373463314000538 Published online by Cambridge University Press

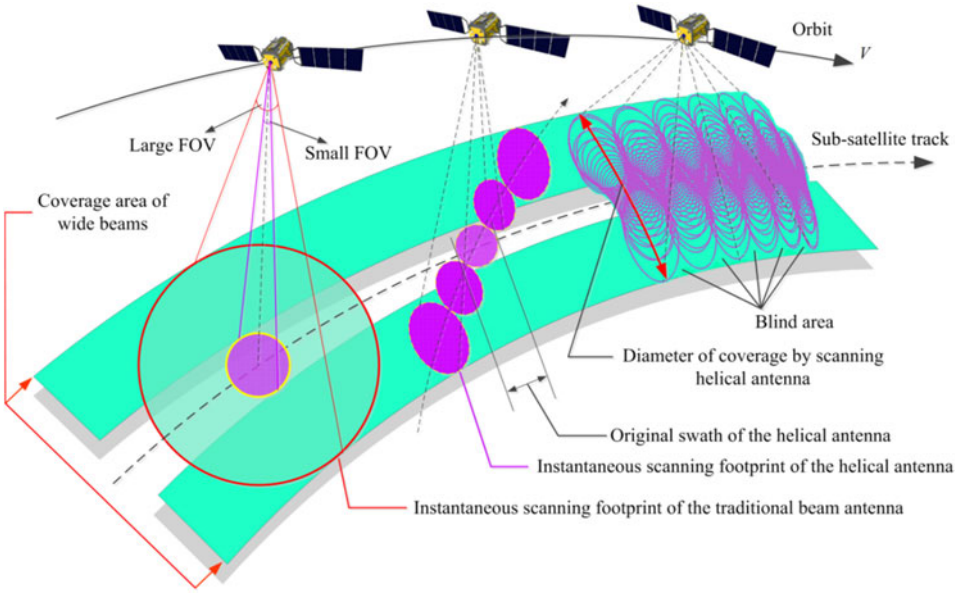

Figure 5. Image of beam scanning based on the helical antenna.

observation times, down to zero on the edge of the satellite FOV in the direction perpendicular to the satellite velocity vector (Cervera et al., 2011). Therefore, in order to achieve complete coverage and account for ship motion between adjacent ascending nodes, the footprints of the antenna in adjacent orbit passes should be overlapped with each other.

The distribution of satellite observation time for all the ships in the footprint of the wide beam antenna is presented in Figure 6. O_1 and O_2 are the sub-satellite points in adjacent orbit passes. The footprints of the antenna partly overlapped across $\widehat{AB}$. The observation time for ships in AB during one single orbit pass is

$$T_{AB}^{obs} = T_{\max}^{obs} \cdot \sin\alpha \tag{11}$$

For this study, the observation time for ships at AB during two adjacent orbit passes is suggested to be no less than T_{max}^{obs} during the two adjacent orbit passes to achieve complete coverage. That means

$$2T_{AB}^{obs} \geqslant T_{max}^{obs} \tag{12}$$

O_1O_2 is the distance between adjacent ascending nodes which can be expressed as

$$L_{O_1O_2} = 2\pi\omega_E R_E \cdot \sqrt{(R_E + H_{sat})^3/\mu} \tag{13}$$

where $R_E = 6378{\cdot}14$ km is the radius of the Earth, $\omega_E = 7{\cdot}29 \times 10^{-5}$ rad/s is the rotation rate of the Earth, $H_{sat} = 600$ km is the orbit height, and $\mu = 3{\cdot}986 \times 10^{14}$ m^3/s^2 is the Earth gravitation constant.

So the swath width of the wide beam antenna is

$$\frac{S_W = 2\widehat{O_1A} = \widehat{O_1O_2}}{\cos\alpha = \dfrac{L_{O_1O_2}}{\cos\alpha}} \tag{14}$$

https://doi.org/10.1017/S0373463314000538 Published online by Cambridge University Press

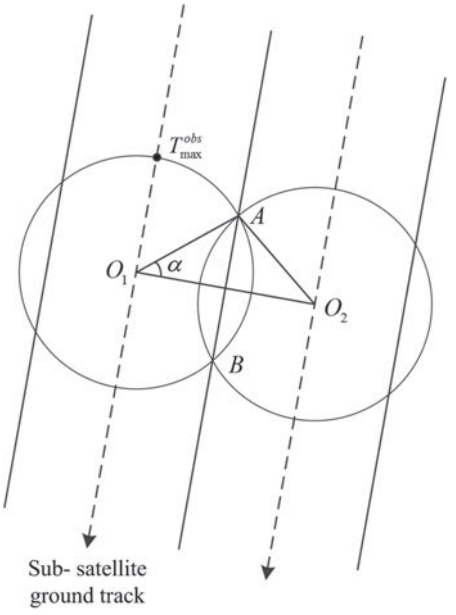

Figure 6. Visualisation of different observation time each ship experiences within the FOV.

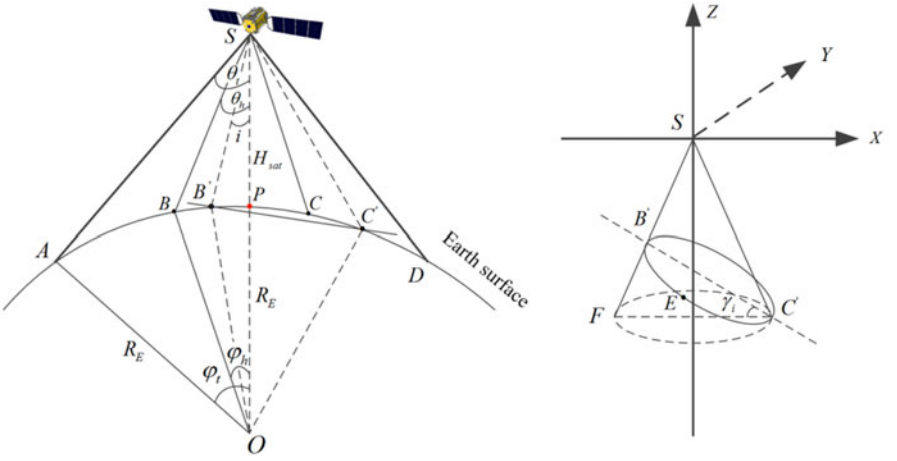

(a) Overview of the observation geometry (b) Partial enlarged picture of the ellipse section

Figure 7. Observation geometry for the beaming scanning method based on the helical antenna.

This is also the swath width that the scanning helical antenna should achieve that determines the side-swaying angle. The detailed process is as follows. Figure 7 shows the observation geometry for the system as viewed from above. The parameters used in Figure 7 have the following meaning: θ_t is half beam width of the wide beam antenna, θ_h is half beam width of the helix antenna and $\widehat{AD}$ is the wide swath. Obviously, the scanning range of the helix antenna should reach $2\theta_t$ so as to obtain the same coverage as the traditional antenna.

https://doi.org/10.1017/S0373463314000538 Published online by Cambridge University Press

The wide swath width in Figure 7 is given by

$$S_W = \widehat{AD} = 2R_E * \varphi_t \tag{15}$$

The angle θ_t can be obtained in the triangle SAO as

$$\frac{R_E}{\sin\theta_t} = \frac{R_E + H_{sat}}{\sin(\theta_t + \varphi_t)} \tag{16}$$

Substituting Equation (13) into Equation (14) yields

$$S_W = \frac{L_{O_1O_2}}{\cos\alpha} = \frac{2\pi\omega_E R_E \cdot \sqrt{(R_E + H_{sat})^3/\mu}}{\cos\alpha} \geqslant \frac{1455{\cdot}7}{\sqrt{3}/2} = 1681 \text{ NM} \tag{17}$$

By combining Equations (15) to (17), the minimum θ_t can be estimated and the value is 62·9°. So the beam width of the traditional antenna S_W is 125·8°.

According to the results in Section 3, the beam width of the helix antenna $2\theta_h$ is designed to be 72·8°. So the side-swaying angle of the scanning helix antenna is

$$\theta_s = \theta_t - \theta_h = 26{\cdot}5° \tag{18}$$

4.3. *The scanning rate*. As viewed from Figure 5, there would be some blind areas at the edge of the coverage during beam scanning if the scanning footprint is tangential in adjacent orbit passes. This is overcome by enlarging the wide swath to make the scanning footprint partly overlap in adjacent orbit passes, as shown in Figure 6. However, there still would be some blind areas inside the coverage because of the high orbit speed. A description of the beam scanning across the wide swath is shown in Figure 8. The three bold dash lines are the adjacent sub-satellite ground track. The circle such as P, P' is the original footprint of the helical antenna and the ellipse such as Q, Q' is the footprint of the helical antenna when scanning at the edge of the wide swath. In one scanning period, the footprint of the helical antenna would vary from Q to Q' in "$Q \rightarrow P \rightarrow Q'' \rightarrow P' \rightarrow Q'$" sequence.

Therefore, in one scanning period, the scanning beam at the edge of the coverage would pass the distance $\widehat{QQ'}$ in the direction parallel to the satellite velocity. To avoid blind areas inside the coverage, the distance $\widehat{QQ'}$ should be shorter than the short axis of the ellipse footprint. The short axis of the ellipse footprint at the edge of the coverage can be estimated in Figure 7(b), expressed as

$$S_a = \frac{2b}{\sqrt{\cot^2\theta_h - \tan^2\gamma_i}} \tag{19}$$

where

$$b = \frac{\widehat{SB'} \cdot \widehat{SC'}}{\widehat{SB'} + \widehat{SC'} \cdot 2\cos\theta_h} \tag{20}$$

$$\tan\gamma_i = \frac{\widehat{SC'} - \widehat{SB'}}{\widehat{SC'} + \widehat{SB'}} \cdot \cot\theta_h \tag{21}$$

https://doi.org/10.1017/S0373463314000538 Published online by Cambridge University Press

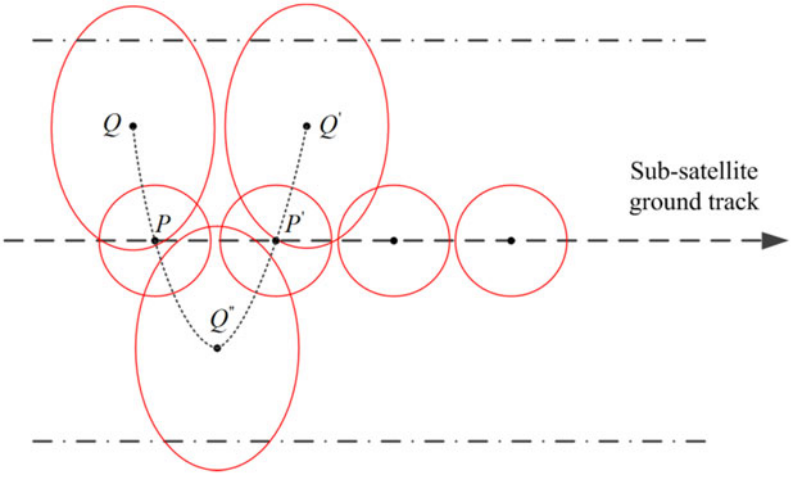

Figure 8. Description of the beam scanning across the wide swath.

And

$$\begin{cases} \widehat{SC'} = \dfrac{R_E \sin\varphi_t}{\sin\theta_t} \\ \widehat{SB'} = (R_E + H_{sat})\cos(2\theta_h - \theta_t) - \sqrt{R_E^2 - [(R_E + H_{sat})\sin(2\theta_h - \theta_t)]^2} \end{cases} \tag{22}$$

Substituting Equation (18) into Equation (22) yields, $\widehat{SC'} = 1732$ km, $\widehat{SB'} = 610$ km.

In a half scanning period, the scanning beam in the middle of the coverage would move from P back to P' with the passing distance $\widehat{PP'}$. To avoid blind areas in this part of the coverage, the distance $\widehat{PP'}$ should be shorter than the original swath of the helical antenna $\widehat{BC}$ (in Figure 7 (a)).

To achieve full coverage, the following equations would be established as the above analyses:

$$\begin{cases} \widehat{QQ'} = v_0 \cdot T_s \leqslant S_a \\ \widehat{PP'} = \dfrac{1}{2} v_0 \cdot T_s \leqslant S_h \end{cases} \tag{23}$$

where, v_0 is the satellite velocity at the 600 km orbit height and T_s is the scanning period of the helical antenna.

The original swath width in Figure 7 is given by

$$S_h = 2 * \widehat{BP} = 2R_E * \varphi_h \tag{24}$$

The angle φ_h in the triangle SBO can be calculated as θ_t by Equation (16)

$$\varphi_h = \arcsin\left((R_E + H_{sat}) \cdot \sin\theta_h / R_E\right) - \theta_h \tag{25}$$

The orbit velocity v_0 is

$$v_0 = R_E \sqrt{\mu / (R_E + H_{sat})^3} \tag{26}$$

https://doi.org/10.1017/S0373463314000538 Published online by Cambridge University Press

Then, the average scanning rate is defined as

$$\omega_s = \frac{4\theta_s}{T_s} \tag{27}$$

Substituting Equation (23) into Equation (27) yields

$$\begin{cases} \omega_s \geqslant \dfrac{4\theta_s \cdot v_0}{S_a} \\ \omega_s \geqslant \dfrac{2\theta_s \cdot v_0}{S_h} \end{cases} \tag{28}$$

And, S_a can be computed by substituting Equations (20) to (22) into Equation (19)

$$S_a = \frac{2b}{\sqrt{\cot^2\theta_h - \tan^2\gamma_i}} = \frac{2 \cdot \dfrac{\widehat{SB'} \cdot \widehat{SC'}}{\widehat{SB'} + \widehat{SC'}} \cdot 2\sin\theta_h}{\sqrt{\cot^2\theta_h - \left(\dfrac{\widehat{SC'}\cos 2\theta_h - \widehat{SB'}}{\widehat{SC'}\sin 2\theta_h}\right)^2}} = 658 \text{ NM} \tag{29}$$

The original swath width S_h given by Equation (24) is

$$S_h = 2 \times \widehat{BP} = 2R_E \cdot \varphi_h = 491 \text{ NM} \tag{30}$$

Finally, the average scanning rate of the helix antenna was evaluated from Equations (27) to (30) as

$$\omega_s \geqslant \frac{2\theta_s \cdot v_0}{S_h} = \frac{2\theta_s \cdot R_E\sqrt{\mu/(R_E + H_{sat})^3}}{S_h} = 0{\cdot}44°/s \tag{31}$$

4.4. *Performance and discussions.* The above analyses have shown that space-based AIS can achieve complete coverage with the traditional wide beam antenna when using a scanning antenna. The ship detection probability based on the scanning antenna still remains to be verified. Compared to the space AIS reception by a fixed antenna in the past, this new scheme has some different characteristics, mainly focusing on the observation time and swath width. When the helical antenna scans across the wide swath, the instantaneous coverage area is changing continuously along with the swaying angle. The visibility of a location on the Earth surface may not be continuous during antenna scanning, which depends on the scanning rate. Therefore, the equivalent coverage area and the equivalent observation time should be evaluated in order to estimate the system performance.

The instantaneous coverage area by this scanning antenna is a spherical ellipse on the Earth surface (Figure 5). The instantaneous beam of the helix antenna is $SB'C'$, as in Figure 7(a). Because the orbit altitude H_{sat} is far less than the Earth radius R_E, the instantaneous coverage area can be viewed as an ellipse section by a plane cutting off a circular cone at an oblique angle. The partial enlarged picture is shown in Figure 7(b). The circular cone $SC'F$ represents the antenna beam and the plane $B'EC'$ is the Earth surface. So the ellipse section $B'EC'$ can be treated as the instantaneous coverage area. This area is determined by combining two equations of the circular

https://doi.org/10.1017/S0373463314000538 Published online by Cambridge University Press

cone and plane as follows

$$\begin{cases} x^2 + y^2 - m^2 z^2 = 0 \\ z = kx + b \end{cases} \tag{32}$$

Then, the instantaneous coverage area can be estimated as

$$A_i = \frac{\pi \cdot b_i^2}{(1/m - m \cdot k_i^2) \cdot \sqrt{(1/m)^2 - k_i^2} \cdot \cos\gamma_i} \tag{33}$$

where, the subscript i signifies that the parameter changes along with the swaying angle i. $m = \tan\theta_h$, $\cos\gamma_i = 1/\sqrt{1 + k_i^2}$ and k_i, b_i can be obtained by the line equation across B' and C'.

Due to symmetry, the equivalent coverage area during one scanning period can be evaluated as

$$\bar{A} = \frac{1}{\theta_s}\int_0^{\theta_S} A_i di = \frac{1}{\theta_s}\int_0^{\theta_S} \frac{\pi b_i^2}{(1/m - m \cdot k_i^2) \cdot \sqrt{(1/m)^2 - k_i^2/2} \cdot \cos\gamma_i} \cdot di \tag{34}$$

Correspondingly, the equivalent swath width is

$$S_{eq} = 2\sqrt{\overline{A}/\pi} \tag{35}$$

By simulations in Matlab, the equivalent swath width is worked out to be 566 NM.

Then, the equivalent observation time can be approximately estimated as

$$\overline{T_{obs}} = T_{obs} \cdot (S_{eq}/S_W)^2 \tag{36}$$

where, T_{obs} is the observation time by a fixed helix antenna of the equivalent swath and S_W is the coverage area of the traditional wide beam antenna.

The ship detection probability as a function of the number of ships using the above beam scanning method is shown in Figure 9. The red curve represents the detection probability by the scanning antenna of the 566 NM equivalent swath. In contrast, the ship detection probability curves under other different equivalent swath widths by this beam scanning method are also plotted in Figure 9. The dark curve represents the detection probability by the traditional antenna with 1681 NM swath width.

As can be seen from Figure 9, the helical antenna with beam scanning has better performance than the fixed traditional wide beam antenna with the same coverage area. For example, with 2000 ships, the detection probability by the fixed antenna of 1681 NM swath is about 70%, while the helix antenna using the beam scanning method can achieve nearly 90%. With the increasing number of ships, the improvement is more obvious. When the number of ships is more than 4000, the detection probability by the fixed antenna decreases rapidly to below 10% but the scanning antenna can still reach 70%. On the whole, the equivalent swath of 566 NM is nearly the optimal swath for its overall shape of the curve when compared with other three cases of the 400 NM, 600 NM and 800 NM equivalent swath.

In addition, the beam scanning method based on the helical antenna has excellent performance in withstanding the ship-reporting interval, shown in Figure 10. The reporting interval has a significant effect on the ship detection probability, which can be seen from Equation (1). For the fixed traditional wide beam antenna of 1681 NM

https://doi.org/10.1017/S0373463314000538 Published online by Cambridge University Press

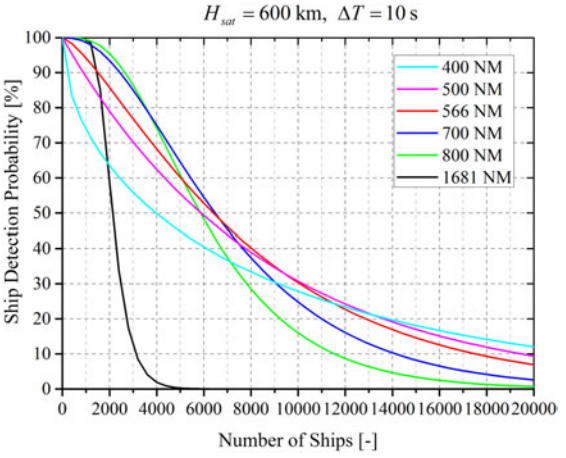

Figure 9. Ship detection probability as a function of number of ships using beam scanning method based on the helix antenna.

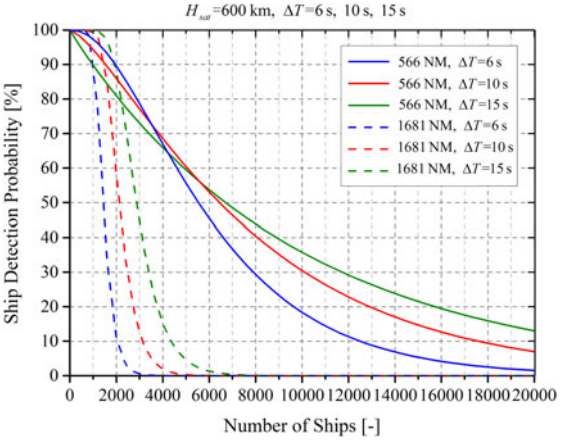

Figure 10. Ship detection probability as a function of number of ships for different reporting intervals.

swath, the ship detection probability decreases sharply from 90% to 60% then to 10% at about 2000 ships as the reporting interval ΔT shortens from 15 s to 10 s and 6 s. When the number of ships is more than 3000, the ship detection probability at $\Delta T = 15$ s drops rapidly from 50% to near zero at $\Delta T = 6$ s. However, by this beam scanning method, the effect of the reporting interval is limited in the beginning of the curve where there are few ships/high ship detection probability. The results in Figure 10 show that the difference in ship detection probability under different reporting intervals is no more than 10% by the 566 NM equivalent swath when the number of ships is less than 6000.

Next, another issue may come up: that of whether the satellite altitude has an effect on the ship detection probability when using this beam scanning method. Generally, a higher altitude means a larger coverage area and a higher number of ships visible

https://doi.org/10.1017/S0373463314000538 Published online by Cambridge University Press

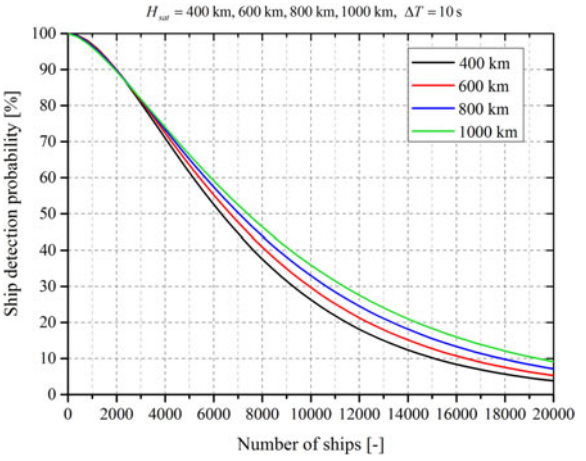

Figure 11. Sensitivity of ship detection probability on the satellite altitude.

but a longer satellite observation time. The near optimal ship detection probability at the altitude of 400 km, 600 km, 800 km and 1000 km by scanning antenna of different swaths is shown in Figure 11. It appears that the 1000 km altitude is a better choice than any others because of its slightly higher ship detection probability at the given large number of ships. However, in real scenarios with constant ship density, the higher altitude would result in a wider swath width, then, there would be more ships in the satellite FOV that pull down the ship detection probability slightly. For example, the required critical swath for a 600 km altitude is 1456 NM and 1584 NM for a 1000 km altitude, then the number of ships would raise from 1860 to about 2200 assuming 1·4 ships per organised cell (as in North Sea/Arctic), and their ship detection probabilities are nearly the same as shown in Figure 11. So the satellite altitude does not have a significant effect on ship detection probability that makes the AIS satellite flexible for piggy-back launches into different orbit heights.

For the real mission scenario in Section 2, the North Sea/Arctic has the highest ship density except for the Mediterranean Sea. The average number of ships in the North Sea/Arctic within coverage of 1681 NM swath is about 2500. Compared with only 20% detection probability by the traditional fixed antenna, this scanning antenna can achieve nearly 80% detection probability. As for the Mediterranean Sea, there will be about 10146 ships to the year 2016 within its coverage of 964 NM diameter. Without considering the sea outline, the ship detection probability can reach $\sim$30% level in one orbit pass when using the scanning antenna, shown in Figure 10. Although this detection probability is not high enough, it is still believed to be valuable progress compared with the near zero detection probability by the fixed traditional wide beam antenna.

5. CONCLUSIONS. In this paper, we propose and investigate a helical antenna and a beam scanning method based on this helical antenna to enhance the ship detection probability and maintain complete coverage of space-based AIS. The preliminary analysis of the results for AIS satellite at the 600 km altitude show these improvements are considerable. Firstly, the narrow beam width helical antenna has

https://doi.org/10.1017/S0373463314000538 Published online by Cambridge University Press

stronger ship detection capacity in high ship density regions and can provide enough gain to improve the strength of the AIS signal and suppress the interference. Secondly, by this beam scanning method, the helical antenna can obtain the same coverage area as the traditional antenna and achieve rapid global ocean covering by just one satellite. More encouragingly, the helical antenna based on this beam scanning method has excellent performance in raising ship detection probability. Also, the detection probability at a moderate number of ships is hardly influenced by the average reporting interval at $\Delta T \leqslant 15$ s. This characteristic can satisfy the ship detection requirements of most oceans without such heavy traffic conditions.

For the real mission scenarios of global ship detection to the year 2016, the proposed scanning antenna shows great detection capacity compared with the fixed traditional wide beam antenna. Even in the Mediterranean Sea, the ship detection probability can still reach the 30% level in one satellite overpass. It can be inferred that based on these improvements, space-based AIS can achieve a higher ship detection probability in one day due to the $2 \sim 3$ times revisit in any region on the Earth.

Although all the above conclusions are drawn on the basis of AIS satellite moving in a 600 km orbit, similar performance can be obtained at different altitudes in LEO. The differences may lie in satellite FOV, the scanning range and the average scanning rate.

In conclusion, the helical antenna and the beam scanning method based on the helical antenna designed in this study is a promising innovation in space-based AIS detection and would be expected to apply in the future space-based AIS system.

Future work may focus on the manufacturing and deployment verification of the large helical antenna on a small satellite platform. In addition, the control law of the antenna scanning should be designed carefully to seek uniform ship covering and minimum energy consumption.

ACKNOWLEDGMENTS

This research has been supported by the National Natural Science Foundation of China under Grant 61302092.

REFERENCES

Block, J., Bäger, A., Behrens, J., Delovski, T., Hauer, L., Schütze, M., Schütze, R. and Spröwitz, T. (2013). A self-deploying and self-stabilizing helical antenna for small satellites. *Acta Astronautica*, **86**, 88–94.

Burzigotti, P., Ginesi, A. and Colavolpe, G. (2012). Advanced receiver design for satellite-based automatic identification system signal detection. *International Journal of Satellite Communications and Networking*, **30**, 52–63.

Carson-Jackson, J. (2012). Satellite AIS – Developing Technology or Existing Capability?. *The Journal of Navigation*, **65**, 303–321.

Cervera, M. A., Ginesi, A. and Eckstein, K. (2011). Satellite-based vessel Automatic Identification System: A feasibility and performance analysis. *International Journal of Satellite Communications and Networking*, **29**, 117–142.

Dahl, O.F.H. (2006). *Space-Based AIS Receiver for Maritime monitoring using interference cancellation*. Master Thesis, Department of Electronics Telecommunications, Norwegian University of Science and Technology.

Dousset, T., Renard, C., Diez, H., Sarrazin, J. and Lepage, A.C. (2012). Compact Patch Antenna for Automatic Identification System (AIS). *The 15th International Symposium on Antenna Technology and Applied Electromagnetics*, Toulouse, France.

ExactEarth. (2013). EV-1 Performance Review. http://www.exactearth.com/media-centre/past-issues-of-exactnews/exactNews-Issue6.pdf. Accessed 20 July 2013.

Gallardo, M. J. and Sorger, U. (2010). Coherent receiver for AIS satellite detection. *Proceedings of the 4th International Symposium on Communications, Control and Signal Processing*, Limassol, Cyprus.

Gunnar Aarsæther, K. and Moan, T. (2009). Estimating Navigation Patterns from AIS, *The Journal of Navigation*, **62**, 587–607.

Høye, G. (2004). Observation Modelling and Detection Probability for Space-based AIS reception—Extended Observation Area. FFI/RAPPORT-2004/04390, Forsvarets Forsknlnginstitutt.

Høye, G. (2006). Space-based AIS-theoretical considerations and system parameter optimization. FFI/RAPPORT-2006/02495, Forsvarets Forsknlnginstitutt.

ITU. (2001). International Telecommunications Union, ITU-R M.1371-1. *Technical Characteristics for a Universal Ship-borne Automatic Identification System Using Time Division Multiple Access in the VHF Maritime Mobile Band*, Geneva, Switzerland.

ITU. (2006). International Telecommunications Union, ITU-R M.2084. *Satellite detection of automatic identification system messages*, Geneva, Switzerland.

Meland, B. J., Narheim, B., Høye, G. and Eriksen, T. (2004). Feasibility Study On Space-Based AIS For Large-Area Surveillance Of Norwegian Waters. FFI/RAPPORT-2004/01190, Forsvarets Forsknlnginstitutt.

Scorzolini, A., De Perini, V., Razzano, E., Colavolpe, G., Mendes, S., Fiori, P. and Sorbo, A. (2010). European enhanced space-based AIS system study. *The 5th Advanced satellite multimedia systems conference and the 11th signal processing for space communications workshop*, Cagliari, Italy.

Silveira, P.A.M., Teixeira, A.P. and Guedes Soares, C. (2013). Use of AIS Data to Characterise Marine Traffic Patterns and Ship Collision Risk off the Coast of Portugal. *The Journal of Navigation*, **66**, 879–898.

Stutzman, W.L. and Thiele, G.A. (2012). *Antenna theory and design, 3ed*. John Wiley & Sons, Inc.

Wahl, T. and Høye, G. K. (2003). New Possible Roles of Small Satellites in Maritime Surveillance. *Proceedings of Fourth IAA Symposium on Small Satellites for Earth Observation*, Berlin, Germany.

Zhang, Z. S., Weinfield, J. and Soni, T. (2010). Combined differential demodulation schemes for satellite-based AIS with GMSK signals. *Proc. Of SPIE 7691, Space Missions and Technologies, 76910C*, Florida, USA.

Zhu, S. Z., Liu, Z., Jiang, W. L. and Guo, K. (2012). The Key technology of Blind Source Separation of Satellite-Based AIS. *Procedia Engineering*, **29**, 3737–3741.